Polarization-Insensitive Angularly Stable Compact Triple Band Stop Frequency Selective Surface for Shielding Electromagnetic Radiations

Juin ACHARJEE [1], Ankita PATHAK [1], Gouri Shankar PAUL [2], Kaushik MANDAL [3]

[1] Dept. of Electronics and Communication Engineering, St. Thomas' College of Engineering & Technology, Kolkata, India
[2] Dept. of Electrical Engineering, Global Institute of Science & Technology, Haldia, 721657, India
[3] Inst. of Radio Physics and Electronics, University of Calcutta, Kolkata, 700009, India

juin.ece@gmail.com, pathakankita9919@gmail.com, gourishankar.paul@gmail.com, kaushikrpe@gmail.com

Submitted January 17, 2023 / Accepted March 28, 2023 / Online first July 31, 2023

Abstract. *A compact single-layer, polarization-insensitive, and angularly stable frequency selective surface (FSS) based multi-stop band filter is reported for shielding three useful frequency bands covering 1.82–2.86 GHz Industrial, scientific, and medical (ISM), 3.52–4.06 GHz Worldwide Interoperability for Microwave Access (WiMAX), and 7.42–8.72 GHz (satellite downlink), centered at 2.4 GHz, 3.6 GHz, and 8.1 GHz, respectively. The proposed unit cell (15 mm × 15 mm) contains four equal-sized square-headed dumbbell (SHD) shaped resonators surrounded by two square ring resonators. The outer and inner square rings offer the first and second stop bands, while the SHD resonators provide the third stop band. A highly polarization-insensitive response is realized owing to the four-fold symmetry in the proposed structure. The unique arrangements of the SHD resonators help to realize higher angular stability under transverse electric (TE), transverse magnetic (TM), and diagonally polarized incident electromagnetic (EM) waves for incidence angles up to 80°, 80°, and 70°, respectively. A detailed analysis in terms of equivalent circuit and parametric variation is carried out to illustrate the higher to lower frequency band ratio. A prototype is fabricated and tested through a proper measurement setup to validate its performance, and it shows good agreement with the simulated results. The proposed FSS unit cell offers better angular stability under diagonally polarised incident waves, attenuation level, minimum higher to lower frequency band ratio, good fractional bandwidth, and compactness. So the designed multi-stopband FSS can be considered a potential candidate for shielding EM radiation across the useful bands.*

Keywords

Frequency selective surface (FSS), polarization-insensitive, angular stability, multi-stopband, square ring, ISM, WiMAX, X-band

1. Introduction

With the rapid development of wireless communication systems, the use of different wireless devices is also increasing enormously. In a wireless communication system, electromagnetic interference (EMI) between several devices becomes a serious issue for system designers. Undesired EMI can degrade system performances. A traditional method like full metallic encloser [1] is often used to protect those sensitive devices from EMI. However, this makes the devices costly and bulky and will also block all possible transmission of EM signals. In such a scenario, FSS plays a vital role by blocking and reflecting EM signals of some specific bands as per the requirements. Traditional FSSs are 2-D arrays of metallic patches or apertures on a dielectric material [1] that can perform bandstop and bandpass filtering, respectively. These characteristics make FSSs suitable for many applications like reduction of radar cross section (RCS), EM shielding, gain enhancement of antennas, reflector for antennas, reduction of mobile phone radiation exposure [2–6], and many more.

Researchers have developed several single-band (stop/pass) FSSs [7–11] during the last decade, and now it is very common. However, the design of multiband FSSs by considering several important issues like miniaturized unit cell, individual control of the closely spaced frequency bands, polarization insensitiveness at all the frequency bands, better angular stability, and minimum band ratio is still a challenging task for the researchers. Shielding of EM signals at two Global System for Mobile Communication (GSM) bands is demonstrated using metallic vias [12] and fractal cross-dipole [13] based FSSs with higher angular stability. A single layer modified double square loop element [14] is used to stop both the X- and Ku-band transmissions. This FSS shows a stable frequency response for the incidence angle up to 60° under the illumination of both the TE and TM polarized waves. A triple band FSS with band-stop at 8.1, 9.8, and 11 GHz is reported in [15]. In [16],

DOI: 10.13164/re.2023.0400

a micro copper mesh-based optically transparent triple-band FSS is reported to pass EM waves at Bluetooth, Wireless Fidelity (Wi-Fi), 4G Long-Term Evolution (LTE), and 5G bands, and its response is fairly stable up to 30° for both TE and TM polarized waves. In [17], a single-layer FSS with angular stability up to 60° is reported to stop frequency bands centered at 4 GHz, 6.95 GHz, and 11.3 GHz. Another single-layer double-sided FSS has been reported in [18] to suppress WiMAX, Wireless Local Area Network (WLAN), and X-band with angular stability up to 50°. In [19], using FSS, another three frequency bands suppression are reported with angular stability up to 75°. In [20], a design of pentaband FSS is reported to suppress 1.5 GHz, 1.8 GHz, 2.5 GHz, 3.5 GHz, and 5.5 GHz bands, and it shows angular stability up to 45°. Unit cell dimension of 0.135 λ_0 is showcased here, whereas measured angular stability is not explored. Very recently, in [21], another design of dual-layer pentaband FSS to suppress Personal Communications Service (PCS), WiFi, Citizens Broadband Radio Service (CBRS), WLAN, and X-band downlink satellite communication band is reported with angular stability up to 54°. Another pentaband FSS is presented in [22] to suppress Global Positioning System (GPS), GSM, Wi-MAX, and WLAN bands using the combination of different loop geometries. There are some recently proposed FSSs [23], [24] that can operate at ultra-wideband and super wideband frequencies. In [23], FSS spans the range of frequencies from 3.04 to 10.88 GHz with 45° of angular stability in both the TE and TM planes of polarisation, whereas in [24], FSS covers the range of frequencies from 3.05 to 35.92 GHz with enough angular stability in both the polarisation planes. It can be inferred from the subsequent literature survey that all the reported articles, whether dual-band, triple band, pentaband, or wideband, had a number of shortcomings. Moreover, to conform with the variable natures of incident EM waves, FSSs should have good stability under TE, TM, and diagonally polarized waves.

To address all these issues, in this work design of a compact four-fold symmetrical FSS is discussed to realize three distinct stop bands at the useful wireless communication bands. The proposed FSS exhibits a smaller higher to lower frequency band ratio (3.37), polarization insensitiveness, and stable transmission characteristics up to 70° angle of incidence when illuminated by different types of polarized EM waves. Initially, two concentric square rings are printed and studied for dual stop bands. Then, the unique placement of four SHD-shaped resonators has been conceived to achieve triple stop band filtering operation with improved shielding effectiveness (SE) under different arrangements. The proposed unit cell has a miniaturized dimension of $0.11\lambda_0 \times 0.11\lambda_0 \times 0.0.01\lambda_0$, λ_0 referring to the free space wavelength at 2.4 GHz. The single-sided and single-layer structure of this proposed FSS minimizes the fabrication complexity. The proposed FSS is fabricated and measured to justify the simulation results. As per the authors' knowledge, this FSS shows maximum stability under the illumination of diagonally polarized EM waves compared to all the related designs discussed so far.

The rest of the article is organized as follows: Section 1 discusses the basics of FSSs followed literature survey. The design methodology of the proposed FSS unit cell geometry is described in Sec. 2. Equivalent circuit model of the proposed structure is discussed in Sec. 3. The polarization insensitivity and angular stability of the proposed structure are verified in Sec. 4. The design parameters are optimized through the parametric analysis of Sec. 5. In Sec. 6, the measured results are compared with the simulation results and the performances of the proposed structure have also been compared with the related works. Finally, the overall conclusions have been made in Sec. 7.

2. Design and Analysis of Proposed Unit Cell Geometry

The schematic diagram of the unit cell structure of the proposed FSS is illustrated in Fig. 1. The unit cell size is 15 mm × 15 mm × 1.6 mm. The proposed cell is realized on a commercially available low-cost FR4 substrate with a height of 1.6 mm, relative permittivity $\varepsilon_r = 4.4$, and loss tangent (tan δ) = 0.02. Finite element method (FEM)-based ANSYS High Frequency Structure Simulator (HFSS) has been used to design the proposed FSS. Three individual elements are taken to suppress the ISM, WiMAX, and X-band downlink satellite communication bands. Stepwise changes in the transmission response (S_{21}) of the proposed FSS with structural modifications are summarized in Fig. 2.

Initially, a single square ring of an overall length of 14.6 mm (λ_0/0.11) and thickness of 0.23 mm is printed on the top surface of the substrate to realize a bandstop response around 2.4 GHz, usable for the ISM band shielding applications. This structure is named Design 1. With proper adjustment of the overall length and width of the square ring, a stop-band of bandwidth 1.04 GHz (1.78–3.06 GHz) is obtained with a maximum attenuation of 38 dB. In the second step (Design 2), another concentric square ring with

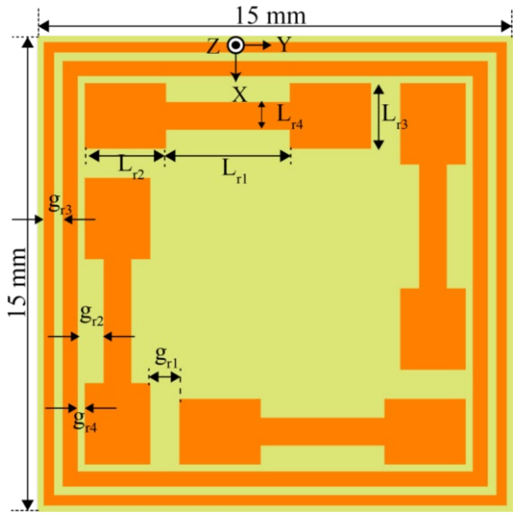

Fig. 1. Unit cell geometry of the proposed FSS. [Optimized parameters: $g_{r1} = 1$; $g_{r2} = 0.9$; $g_{r3} = 0.23$; $g_{r4} = 0.3$; $L_{r1} = 4$; $L_{r2} = L_{r3} = 2.5$; $L_{r4} = 0.8$ (all dimensions are in mm)].

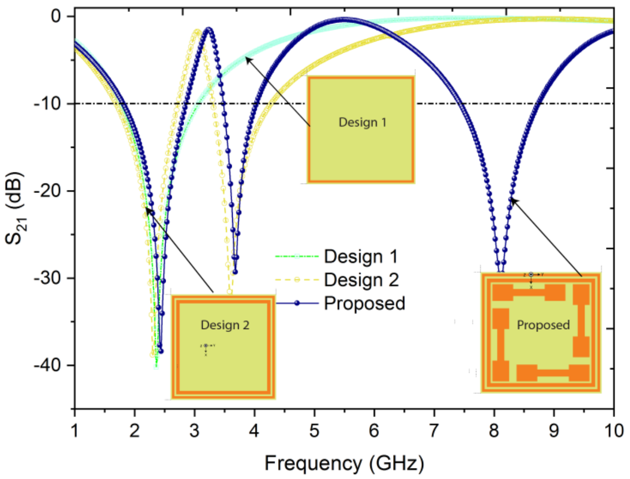

Fig. 2. Stepwise improvement in transmission characteristics (S_{21}) with the structural modifications in the unit cell of the proposed FSS.

an overall length of 13.4 mm (λ_0/0.16) and width of 0.4 mm is incorporated with the previous design to mitigate the transmission of WiMAX band (3.32–4.28 GHz) signals with a resonating frequency of 3.6 GHz.

This structural modification slightly shifts the resonance point of the first stop-band, but the overall band remains almost unchanged. In the final stage of the modification of the structure, four similar-sized square-headed dumbbell (SHD) shaped resonators have been included within the premises surrounded by the square rings. This structural modification has been conceived to mitigate the transmission of EM signals at the X-band downlink satellite communication band (7.4 GHz to 8.7 GHz). Hence, the infinite array analysis of this proposed FSS unit cell consists of four similar SHD-shaped resonators surrounded by two concentric square rings that provide band-stop response at three useful wireless bands (1.82–2.86 GHz, 3.48–4.04 GHz, and 7.44–8.74 GHz) with good attenuation levels at all three bands, as shown in Fig. 2. The stability and SE of the third band have gradually increased due to the contribution of all four SHD-shaped resonators together. This insertion also converts the third band from being two separated, closely lying small bands to a wideband with good impedance matching.

3. Equivalent Circuit Model

This section presents the lumped circuit model analysis and their responses for the proposed triple band-stop FSS, which are shown in Fig. 3. Transmission line theory is adopted for the development of an equivalent circuit model (ECM) of the proposed unit cell of FSS. Since the proposed FSS exhibits bandstop response in three bands due to the three sets of resonators, there will be three different resonating elements in the ECM. Each resonating element is modeled using a series combination of an inductor (L) and a capacitor (C). Therefore, in the ECM (Fig. 3a), three sets of LC are drawn in parallel. The free space impedance (377 Ω) is connected at both ends of the circuit to realize the characteristic impedance (Z_0) of the transmission line. The impedance of the n^{th} LC resonator is calculated using (1), as discussed in [22].

$$Z_n = \mathrm{j}\omega L_n + \frac{1}{\mathrm{j}\omega C_n} \tag{1}$$

where $n = 1, 2, 3$, $\mathrm{j}\omega L_n$ and $1/(\mathrm{j}\omega C_n)$ are the individual impedance associated with inductance and capacitance of LC resonator. By simplifying (1), it can be represented by (2)

$$Z_n = \frac{1-\omega^2 L_n C_n}{\mathrm{j}\omega C_n}. \tag{2}$$

To find out the transmission zeros at the corresponding resonating frequencies, the numerator of (2) is made equal to 0 and the calculated values of L and C for all the branches of the ECM (Fig. 3a) are L_1 = 4 nH, C_1 = 1.128 pF, L_2 = 3 nH, C_2 = 0.63 pF, and L_3 = 1 nH, and C_3 = 0.388 pF for the frequencies 2.4 GHz, 3.6 GHz, and 8.1 GHz, respectively. Actually, there are no closed-form expressions to determine the inductance (L) and capacitance (C) values of such a complicated FSS topology. Hence, we have considered two well-known empirical formulas to determine the initial values of L and C, and afterward, the parameters are fine-tuned using the Advanced Design System (ADS) software using the curve tracing method. The circuit is designed and simulated on the ADS platform and also optimized to obtain the equivalent circuit response, as illustrated in Fig. 3(b). Figure 3(b) shows the comparison of the responses of full-wave simulation and ECM simulation, and they are in good agreement. No changes in resonating frequencies are observed, but a slight mismatch in the operating bands generally arises for not considering the mutual

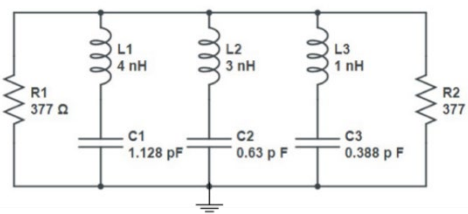

(a)

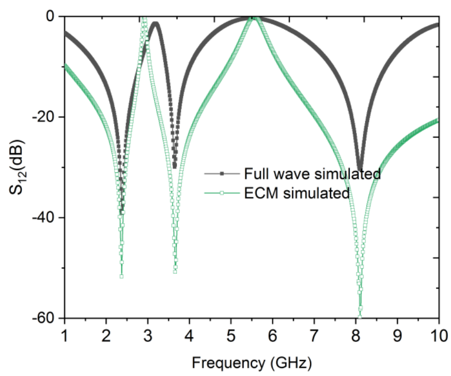

(b)

Fig. 3. (a) Equivalent circuit model of the unit cell of the proposed FSS. (b) Comparison of full-wave simulation with equivalent circuit simulation.

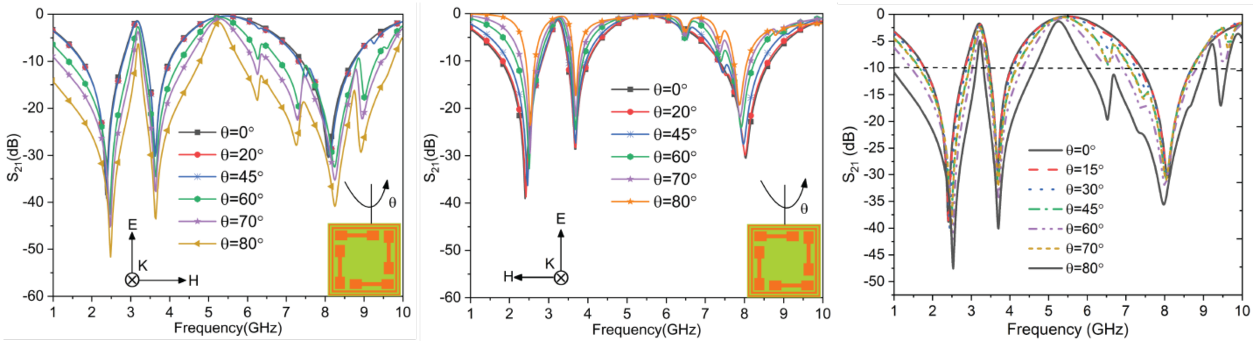

(a) (b) (c)

Fig. 4. Variation in transmission characteristics for different incidence angles under (a) TE polarization, (b) TM polarization, and (c) diagonal polarization.

effect between the resonating elements, which are closely spaced to make the design compact.

4. Angular Stability and Polarization Insensitiveness

FSS, as installed for a particular application, could be illuminated by various EM waves with different polarizations and incidence angles. Therefore it is essential to examine the transmission response of the proposed FSS for different incidence angles under different polarizations. These analyses on angular stability under TE, TM, and diagonal ($\phi = 45°$) conditions are summarized in Fig. 4 for the variation of incidence angles up to 80°. It is observed that for incidence angles up to 60°, there is no such deviation in resonating frequencies and operating bands for all three bands under all polarization states. For an incidence angle ≥70°, a slight shift in resonating frequencies and enhancement in bandwidth have been observed, particularly in the third operating band. The desired stop-band resonating frequency is not changing till the 80° angle of incidence under both the TE and TM modes and till 70° for diagonally polarized incident waves. Therefore, the slight enhancement in bandwidth can be suitably neglected, and angular stability of 80° under TE, 80° under TM, and 70° under diagonally polarized incident waves can be claimed for this proposed FSS. To check the polarization insensitiveness of the proposed FSS, the transmission response has been checked under the normal incidence of EM waves for different polarizations. This analysis is shown in Fig. 5. For all possible polarizations of the incident EM waves, the transmission response of the proposed structure remains unchanged for all three operating bands. Hence, the proposed FSS is completely polarization-insensitive. The induced surface current distributions on the proposed unit cell at three desired frequencies are shown in Fig. 6 to elaborate the physical insight into the underlying resonance mechanism. It shows that current concentration is stronger along the outer square ring, inner square ring, and SHD-shaped resonators at 2.44 GHz, 3.68 GHz, and 8.1 GHz, respectively. The placement of four SHD resonators in the vicinity of the inner ring develops mutual coupling, resulting in small induction of the current flow at two resonators at 3.68 GHz. This study confirms that the resonators with a higher periphery are responsible for the stop-band response at a lower frequency.

5. Parametric Analysis

To make the dimension of the unit cell compact, the spacing between the elements has to be too small, which can cause coupling between them and degrade the SE. Further, to ensure the usefulness of the proposed FSS for the closely spaced frequency bands, the frequency band ratio also needs to be maintained at lower values. Therefore, some sensible design parameters like the thickness of

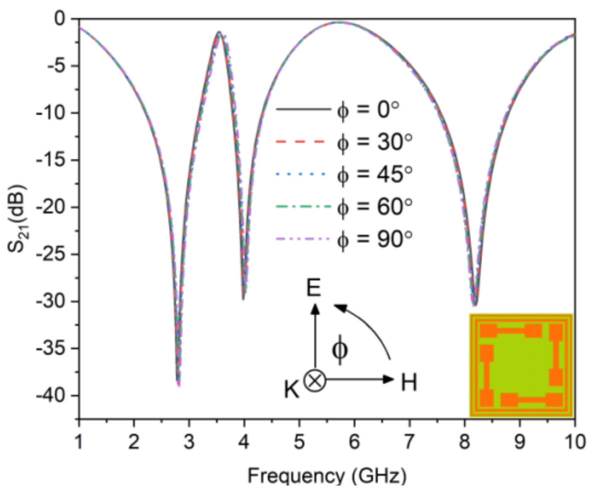

Fig. 5. Effect on transmission characteristics for variations in polarization angles under normal incidence.

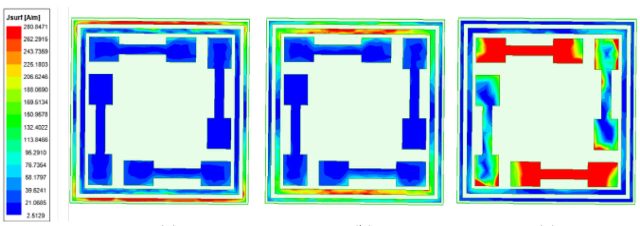

(a) (b) (c)

Fig. 6. Simulated surface current distribution on the proposed unit cell at (a) 2.44 GHz, (b) 3.68 GHz, and (c) 8.1 GHz.

the outer square ring, the spacing between the square ring resonators, and the number of SHD resonators are varied, and the corresponding stop-band frequency responses are checked, optimized, and analyzed thoroughly.

5.1 Thickness Variation of Outer Square Ring Resonator

The overall length and thickness of the outer square ring were chosen to realize a stop-band response across the ISM band (1.78–3.06 GHz). With the variation in thickness of this outer square ring, only the first operating band is shifted towards the lower frequency, as shown in Fig. 7. However, the other two operating bands remain unchanged. The outer square ring thickness is finalized at 0.23 mm. This analysis confirms the main advantage (every operating bands can be tuned independently) of the proposed FSS.

5.2 Variation of Spacing between the Square Ring Resonators

Variation of the gap between the ring resonators mainly affects the position of the second and third operating bands, as shown in Fig. 8(a). As the gap widens, the second and third operating bands become closer, and the SE deteriorates in these two bands. In the case of a smaller gap, two bands become more apart without much affecting the SE. Therefore the optimized gap between the square ring resonators is kept at 0.35 mm by considering both the requirements of the desired frequency band and good SE across the operating bands.

5.3 Variation of Number of SHD-Shaped Resonators

The proper placement and the total number of SHD-shaped resonators are crucial for achieving the third operating band with good shielding ability, as shown in Fig. 8(b). The unit cell with two horizontal SHD-shaped resonators or with two vertical SHD-shaped resonators is not able to concentrate the electric fields for generating a new resonance and also affects the first two operating bands. However, the strategic arrangement of four SHD-shaped resonators produces a new resonance at the desired frequency range. This unique arrangement of four SHD-shaped resonators makes the proposed unit cell four-fold symmetric, which helps in achieving maximum SE along with polarization insensitivity.

5.4 Variation of Overall Dimension of SHD-Shaped Resonators

Variation of the overall dimension of all dumbbells mainly affects the third resonating band. The impact on the other two resonant bands is minimal. Moreover, the performance is tested only for a few variations of resonator dimensions due to the limited scope for size enhancement. Through the parametric studies, all the dimensions of the FSS are optimized, and obtained frequency band ratios in the three operating bands are 1.5 (f_2/f_1), 2.25 (f_3/f_2), and 3.3 (f_3/f_1), respectively. The minimum band ratio confirms the applicability of the proposed FSS for rejecting closely spaced frequency bands.

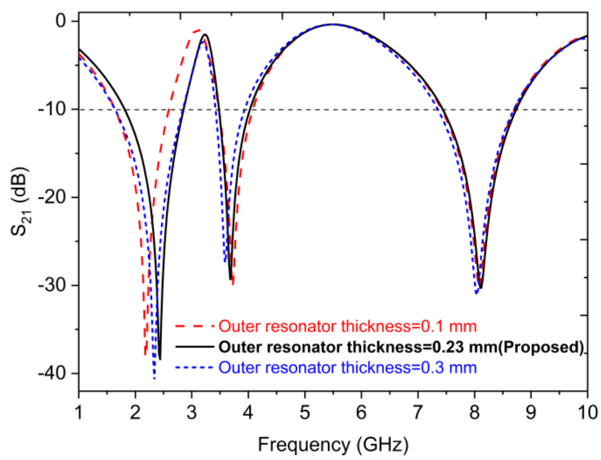

Fig. 7. Effect on S_{21} for the variation of thickness of outer square resonator.

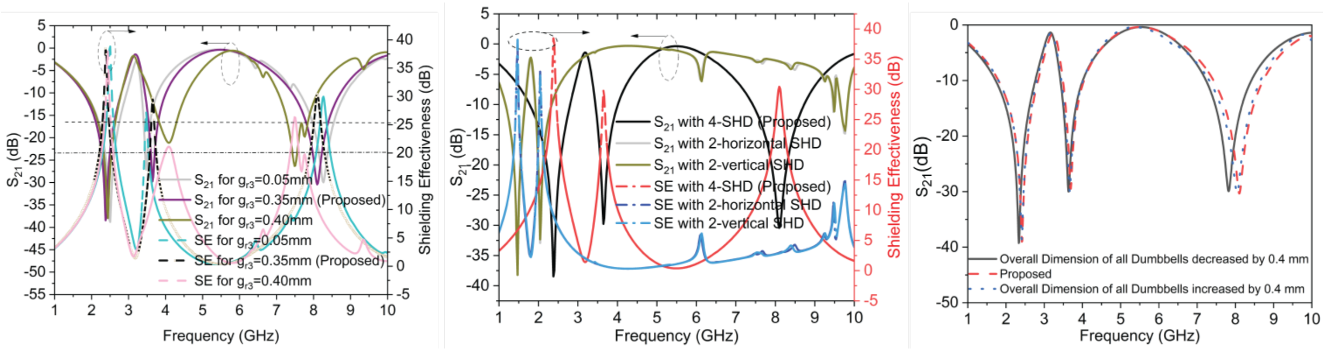

(a) (b) (c)

Fig. 8. Effect on S_{21} and SE for the variation of (a) gap between the two square ring resonators and (b) variation of number of SHD-shaped resonators. (c) S_{21} effects for the variation of overall dimension of all dumbbells.

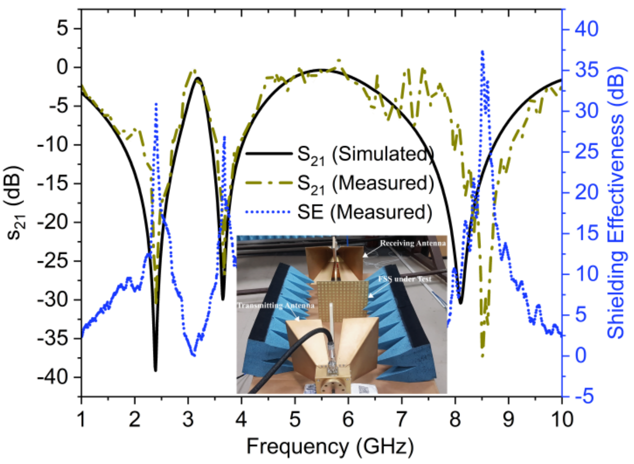

Fig. 9. Comparison of simulated and measured S_{21} curves for the proposed FSS.

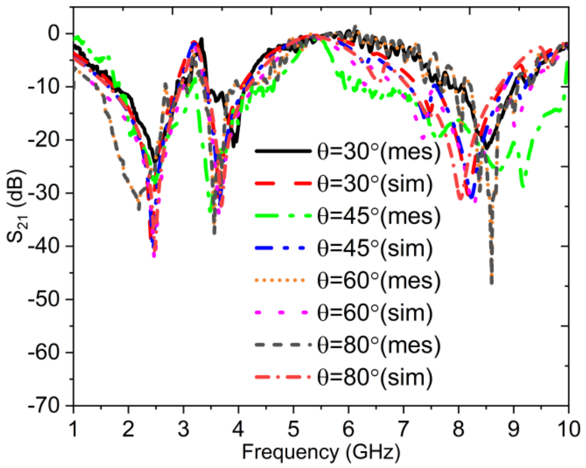

Fig. 10. Comparison of simulated and measured S_{21} for different incidence angles under TE mode.

6. Measurement Results and Discussion

The prototype of the proposed FSS is fabricated with a 14 × 14 unit cell, which occupies an overall dimension of 210 × 210 mm^2. The transmission coefficients of the proposed FSS for normal and oblique incidence of EM waves under TE mode are measured using a proper measurement setup. A comparison between simulated and measured S_{21} along with the SE plots are shown in Fig. 9. A photograph of the FSS under test is also shown in the inset of Fig. 9. The measured S_{21} shows < -10 dB stop-band across three operating bands at 2.16–2.7 GHz (22.5%), 3.54–3.97 GHz (11.68%), and 7.96–9.04 GHz (13.33%) with maximum attenuation level 31 dB, 26 dB, and 38 dB, respectively. There are negligible dissimilarities between the results, due to some fabrication limitations. Figure 10 shows the comparison between simulated and measured S_{21} for different incidence angles under TE mode. For oblique incidence, a slight variation in the resonating point is observed in some cases, but the overall operating band remains almost constant. Scattering is mainly observed in the higher frequency band due to edge diffraction [16]. Due to some measurement limitations, incidence angle variations under TM mode were not checked.

In the measurement system, the FSS was maintained between two identical linearly polarised broadband antennas (operating range: 450 MHz–18 GHz), one of which

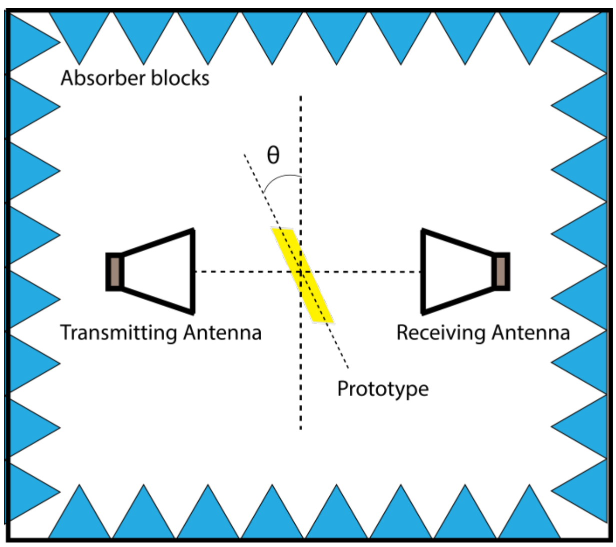

Fig. 11. Schematic diagram of measurement setup.

Ref. No.	Dimension of unit cell	No. of stop-bands	Operating frequency	Fractional BW (%)	Stability under diagonally polarized incidence	Frequency ratio (Higher to lower resonance)	Maximum attenuation
[12]	$0.048\lambda_0 \times 0.048\lambda_0$	2	900, 1800 MHz	10, 10	NM	2	close to 70 dB
[15]	$0.55\lambda_0 \times 0.55\lambda_0$	3	8.1, 9.8, 11 GHz	15, 13, 18	NM	1.35	close to 36 dB
[16]	$0.2\lambda_0 \times 0.2\lambda_0$	3	2.4, 3.7, 5.7 GHz	NM, 5.40, 7	NM	2.375	35 dB
[17]	$0.091\lambda_0 \times 0.091\lambda_0$	3	4, 6.95, 11.3 GHz	13.9, 25, 6.9	NM	2.82	≈ 40 dB
[18]	$0.10\lambda_0 \times 0.10\lambda_0$	3	3.5, 5.2, 10.2 GHz	14.4, 37.6, 40	NM	2.91	up to 35 dB
[19]	$0.125\lambda_0 \times 0.125\lambda_0$	3	2.5, 3.5, 5.5 GHz.	44, 8, 31	NM	2.2	up to 36 dB
This work	$0.11\lambda_0 \times 0.11\lambda_0$	3	2.4, 3.6, 8.1 GHz	22.5, 11.68, 13.33	70°	3.3	≈ 40 dB

NM: Not mentioned

Tab. 1. Performance comparison of the proposed FSS with similar type of work.

serves as a transmitter and the other as a receiver, that was placed in the far field. The photo of the measurement setup is shown in the inset of Fig. 9 and the schematic diagram of measurement setup is shown in Fig. 11. During the measurement under oblique incidence, the antennas were kept fixed, whereas the prototype was rotated with respect to its axis to measure the oblique incidence response.

Slight dissimilarities between the simulated and measured S_{21} may be due to comparing the result of an infinite array (simulation) and finite array (fabricated FSS). To prove the effectiveness of the proposed FSS, a comparison is made with other recently published similar works in terms of unit cell size, the number of operating bands, polarization insensitivity, degree of angular stability, shielding effectiveness, and attenuation level. This comparative study is summarized in Tab. 1. The proposed FSS offers maximum angular stability (70°) under diagonally polarized incidence waves compared to all the related designs [16–19] while maintaining a better frequency band ratio. The structure is compact and provides maximum attenuation compared to all designs except a dual-band FSS [12]. Moreover, being a single-layer, single-sided structure, it makes the fabrication job easier. Therefore, compared to the other reported structures, the proposed FSS unit cell provides a suitable trade-off among angular stability under diagonally polarized incidence waves, attenuation level, minimum higher to lower frequency band ratio, and compactness.

7. Conclusion

A miniaturized, polarization-insensitive, four-fold symmetrical FSS unit cell structure has been designed and studied in this work. Four equal-sized SHD-shaped resonators surrounded by two square ring resonators are conceived for achieving triple stop band filtering operation with improved shielding effectiveness. Surface current distributions on different resonators at different frequencies prove the lower mutual coupling between the resonators. To further elaborate the operation mechanism a lumped circuit model is derived and its outcome shows good agreement with the simulated one. This FSS shows stable reflection performances over a wide range of incidence angles for TE, TM, and diagonally polarized incident waves. A smaller higher to lower stop band ratio compared to the other reported triple band FSSs confirms the effectiveness of the proposed FSS for shielding closely spaced frequency bands. The measured and simulated results show good agreement between them. The structure can be modified easily by the tactical inclusion of a few more resonators to increase the number of stop bands while maintaining the other parameters unchanged. This FSS can be installed in various areas, like hospitals and military areas, to shield the corresponding regions from unwanted EM radiations.

Acknowledgment

The authors would like to acknowledge Dr. Saptarshi Ghosh, Indian Institute of Technology Indore, Madhya Pradesh, India, for providing measurement facilities.

References

[1] MUNK, B. A. *Frequency Selective Surfaces: Theory and Design.* 1st ed. John Wiley & Sons, 2005. ISBN: 978-0471370475

[2] THUMMALURU, S. R., KUMAR, R., CHAUDHARY, R. K. Isolation enhancement and radar cross section reduction of MIMO antenna with frequency selective surface. *IEEE Transactions on Antennas and Propagation,* 2018, vol. 66, no. 3, p. 1595–1600. DOI: 10.1109/TAP.2018.2794417

[3] GHOSH, S., SRIVASTAVA, K. V. Broadband polarization-insensitive tunable frequency selective surface for wideband shielding. *IEEE Transactions on Electromagnetic Compatibility,* 2018, vol. 60, no. 1, p. 166–172. DOI: 10.1109/TEMC.2017.2706359

[4] DAS, P., MANDAL, K. Modelling of ultra-wide stop-band frequency-selective surface to enhance the gain of a UWB antenna. *IET Microwaves, Antennas & Propagation,* 2019, vol. 13, no. 3, p. 269–277. DOI: 10.1049/iet-map.2018.5426

[5] YUAN, Y., XI, X., ZHAO, Y. Compact UWB FSS reflector for antenna gain enhancement. *IET Microwaves, Antennas & Propagation,* 2019, vol. 13, no. 10, p. 1749–1755. DOI: 10.1049/iet-map.2019.0083

[6] PAUL, G. S., MANDAL, K., ACHARJEE, J., et al. Reduction of mobile phone radiation exposure using multi-stopband frequency selective surface. *Progress in Electromagnetic Research-M,* 2019, vol. 83, p. 9–18. DOI: 10.2528/PIERM19041401

[7] PAUL, G. S., MANDAL, K., DAS, P. Low profile polarization-insensitive wide stop-band frequency selective surface with effective electromagnetic shielding. *International Journal of RF and Microwave Computer-Aided Engineering,* 2021, vol. 31, no. 3, p. 1–8. DOI: 10.1002/mmce.22527

[8] PAUL, G. S., MANDAL, K. Polarization-insensitive and angularly stable compact ultrawide stop-band frequency selective surface. *IEEE Antennas and Wireless Propagation Letters,* 2019, vol. 18, no. 9, p. 1917–1921. DOI: 10.1109/LAWP.2019.2933545

[9] TANG, Z., ZHAN, J., ZHONG, B., et al. An ultrawideband frequency selective surface with high stability for electromagnetic stealth. *Journal of Electromagnetic Waves and Applications,* 2021, vol. 36, no. 1, p. 141–153. DOI: 10.1080/09205071.2021.1958703

[10] KANCHANA, D., RADHA, S., SREEJA, S. A single layer UWB frequency selective surface for shielding supplication. *Journal of Electronic Materials,* 2020, vol. 49, p. 4794–4800. DOI: 10.1007/s11664-020-08210-x

[11] KATOCH, K., JAGLAN, N., GUPTA, S. D., et al. Design of a triple band notched polarization independent compact FSS at UWB frequency range. *International Journal of RF and Microwave Computer-Aided Engineering,* 2021, vol. 31, no. 6, p. 1–14. DOI: 10.1002/mmce.22631

[12] XU, X. M. A compact angularly-stable frequency selective surface for GSM 900/1800-MHz shielding using cascaded 2.5-dimension structure. *International Journal of RF and Microwave Computer-Aided Engineering,* 2018, vol. 29, no. 6, p. 1–7. DOI: 10.1002/mmce.21682

[13] YANG, Y., LI, W., SALAMA, K. N., et al. Polarization insensitive and transparent frequency selective surface for dual band GSM shielding. *IEEE Transactions on Antennas and Propagation,* 2021, vol. 69, no. 5, p. 2779–2789. DOI: 10.1109/TAP.2020.3032827

[14] KANCHANA, D., RADHA, S., SREEJA, B. S., et al. A miniaturized flexible frequency selective surface for dual band response. *International Journal of Microwave and Wireless Technologies,* 2020, vol. 13, p. 810–816. DOI: 10.1017/S1759078720001506

[15] MAHAVEER, U., CHANDRASEKARAN, K. T., MOHAN, M. P., et al. A tri-band frequency-selective surface. *Journal of Electromagnetic Waves and Applications,* 2021, vol. 35, no. 7, p. 861–873. DOI: 10.1080/09205071.2020.1865206

[16] SHARMA, S. K., ZHOU, D., LUTTGEN, A. C., et al. A micro copper mesh-based optically transparent triple band frequency selective surface. *IEEE Antennas and Wireless Propagation Letters,* 2019, vol. 18, no. 1, p. 202–206. DOI: 10.1109/LAWP.2018.2886305

[17] DEY, S., DEY, S. Conformal miniaturized angular stable triband frequency selective surface for EMI shielding. *IEEE Transactions on Electromagnetic Compatibility*, 2022, vol. 64, no. 4, p. 1031 to 1041. DOI: 10.1109/TEMC.2022.3153998

[18] BASHIRI, M., GHOBADI, C., NOURINIA, J., et al. WiMAX, WLAN, and X-band filtering mechanism: Simple-structured triple-band frequency selective surface. *IEEE Antennas and Wireless Propagation Letters*, 2017, vol. 16, p. 3245–3248. DOI: 10.1109/lawp.2017.2771265

[19] GARG, S., YADAV, S., ASERI, K., et al. A novel reflective frequency selective surface for triple frequency applications. In *International Conference on Computing, Communication and Automation (ICCCA)*. Greater Noida (India), 2017, p. 1522–1525. DOI: 10.1109/CCAA.2017.8230043

[20] YADAV, S., JAIN, C. P., SHARMA, M. M. Smartphone frequency shielding with penta-bandstop FSS for security and electromagnetic health applications. *IEEE Transactions on Electromagnetic Compatibility,* 2019, vol. 61, no. 3, p. 887–892. DOI: 10.1109/TEMC.2018.2839707

[21] GHOSH, A., KUMAR, M., ISLAM, S. N., et al. Design and analysis of a compact penta-band polarization-insensitive bandstop frequency selective surface. *IEEE Antennas and Wireless Propagation Letters,* 2020, vol. 19, no. 1, p. 59–63. DOI: 10.1109/LAWP.2019.2952689

[22] FAROOQ, U., IFTIKHAR, A., SHAFIQUE, M. F., et al. Polarization insensitive penta-bandstop frequency selective surface for closely placed bands. *Microwave and Optical Technology Letters,* 2021, vol. 63, no. 1, p. 271–278. DOI: 10.1002/mop.32571

[23] KUNDU, S., CHATTERJEE, A. A compact super wideband antenna with stable and improved radiation using super wideband frequency selective surface. *AEU - International Journal of Electronics and Communications*, 2022, vol. 150, p. 1–12. DOI: 10.1016/j.aeue.2022.154200

[24] KUNDU, S., CHATTERJEE, A. A new compact ultra-wideband frequency selective surface with angular stability and polarization independence for antenna radiation enhancement in microwave imaging application. *AEU - International Journal of Electronics and Communications*, 2022, vol. 155, p. 1–12. DOI: 10.1016/j.aeue.2022.154351

About the Authors …

Juin ACHARJEE (corresponding author) received her Ph.D. from the National Institute of Technology, Durgapur in July 2020. Since 2018, she has been working as an Assistant Professor in the Dept. of ECE, ST. Thomas' College of Engineering and Technology, Kolkata, West Bengal. She has authored or co-authored more than 20 internationally refereed journal papers along with an international patent. Her current research interests include the design of circularly polarized antennas, MIMO antennas for sub-6 GHz applications, and performance enhancement of microstrip antennas using frequency selective surface (FSS), microwave absorbers. Dr. Acharjee is a member of IEEE.

Ankita PATHAK graduate with B.Tech. degree in Electronics and Communication Engineering from St. Thomas's College of Engineering and Technology, Kolkata, India, in 2021 under the affiliation of former West Bengal University of Technology, later MAKAUT. She is currently pursuing Masters of Science degree in Information and Communication Technology with Networks and Digital Communication as her major from October 2022 at Friedrich-Alexander-Universität (FAU) Erlangen-Nürnberg, in the Bayern, Germany. Her research areas include vehicular communication, 4G/5G/6G applications and PQoS, and multiband frequency selective surfaces.

Gouri Shankar PAUL received his B.Tech. degree in Electronics and Communication Engineering from Haldia Institute of Technology, West Bengal, India, in 2009 under the affiliation of former West Bengal University of Technology, and M.Tech. degree in Radio Physics and Electronics in 2018 and from the Institute of Radio Physics and Electronics, Calcutta University, India. He is currently pursuing his Ph.D. degree at the Institute of Radio Physics and Electronics, University of Calcutta, West Bengal, India. Since 2011 he is working as an Assistant Professor in the Electrical Engineering Dept. in Global Institute of Science and Technology, ICARE, Haldia, West Bengal, India. His research areas include analysis and design of various wideband and multiband frequency selective surfaces.

Kaushik MANDAL received his B.Sc degree in Physics (H), B.Tech, and M.Tech degrees in Radio Physics and Electronics from the University of Calcutta, in 2001, 2004, and 2006, respectively. He received his Ph.D. (Tech.) from the University of Kalyani, in July 2014. Since 2016 he is working as an Assistant Professor at the Institute of Radio Physics and Electronics, University of Calcutta, West Bengal, India. He has authored or co-authored 54 internationally refereed journal papers along with an international patent. His current research interests include the design of circularly polarized antennas, SIW integrated microstrip antennas, MIMO antennas for sub-6 GHz applications, and performance enhancement of microstrip antennas using frequency selective surface (FSS) and metamaterial. Dr. Mandal is a senior member of IEEE. He served as the Secretary of IEEE AP-MTT Chapter, Kolkata Section for the years 2020, 2021 and 2023.